Proceedings of 2004 JUSFA
2004 Japan – USA Symposium on Flexible Automation
Denver, Colorado, July 19-21, 2004

UL_054

SPEED CONTROL AND POSITION ESTIMATION OF SMALL HYDRAULIC CYLINDERS FOR DIGITAL CLAY USING PWM METHOD

Haihong Zhu
Woodruff School of Mechanical Engineering
Georgia Institute of Technology
Atlanta GA 30332-0405 USA

Wayne J. Book
Woodruff School of Mechanical Engineering
Georgia Institute of Technology
Atlanta GA 30332-0405 USA

ABSTRACT

Digital Clay is a novel 3D computer input and output device for surface shape and haptic effects. The device consists of arrays of fluidically actuated cells under the control of valves connected to two pressure reservoirs in a manner ultimately suitable to an implementation in MEMS technology. At the current stage, it is very difficult to implement a tiny position sensor into each tiny cell. This paper presents a method of speed control and position estimation for the cells of digital clay using only low cost pressure sensors without any position-sensing device.

Keywords: digital clay, PWM, speed control, position estimation

1. INTRODUCTION

Shape is a key element in successful communication, interpretation, and understanding of complex data in virtually every area of engineering, art, science, and medicine. Digital Clay is a novel haptic computer interface that will enable both user-specified display of shapes as output from a computer, and the user-directed input of shapes to a computer. It is named because, like ordinary clay, Digital Clay will allow an area of moderate size to be touched, reshaped with pressure, and seen by the user in a three-dimensional form as illustrated in Figure 1-1. However, beyond ordinary clay, Digital Clay also provides parameters to the computer that will represent the shape to the computer for further analysis, storage, replication, communication and/or modification. Digital Clay will also allow the computer to prescribe its shape as also portrayed in Figure 1-1. Note that figure 1-1 only gives a concept of the Digital Clay. The final structure may be different but the function will stay the same.

Digital Clay comprises an instrumented, actuated, computer-interfaced physical volume bounded by an actuatable surface that acts as the haptic interface. This surface is displaced by arrays of controllable interconnected fluidic-driven actuators which together act to convey the surface topography of 3D or 2.5D objects by means of manipulation of a scaffold internal to the volume of the clay. Each actuator comprises a discrete fluidically inflatable cell that is connected to two common pressurized reservoirs (within a base) through two dedicated two-way miniature valves. Ultimately each valve will be integrated with a pressure sensor, manufactured by MEMS technology that is under development at Georgia Tech.

Figure 1-1 Digital Clay Concept

Digital Clay's control will be organized into three levels. The top application level is represented by application programming interface (API) software that generates commands to the surface control level. The next level, surface control, considers cell-cell interaction and commands actuation of the cell control level. The bottom level, cell control, incorporates sensor feedback to drive individual valves in response to commands and sensed pressure.

This paper focuses on the speed and position control of discrete actuators connected to two pressure reservoirs by simple on/off solenoid valves of variable restriction intended to achieve the functions necessary for the ultimate digital clay. Simple on/off valves are cheap and easy to implement using MEMS technology. However, they are difficult to control to achieve desired flow rate precisely by conventional methods. Research showed that it is possible to combine several on/off valves to achieve flow rate control [1]. Other research showed that with the feedback from the valve's plunger, the PWM (Pulse Width Modulation) method can get a good flow and pressure control [2]. Other research showed that the PWM method can achieve a rough flow rate control with limited flow rate control range [3] [4] [5]. These solutions are not suitable for Digital Clay since they either need multi valves [1] or position feedback from the valve's plunger [2], or the variation of pressure at some valve inputs reduces the accuracy[3][4][5]. Moreover, most research mentioned above focuses on pneumatic systems.

Another challenge is to get position feedbacks from tiny cells (1 to 3 mm in diameter). There are technologies that use the pressure across the valve to estimate the fluid volume passing through the orifice of the valve. However, the pressure variation is very big when the valve turns on and off, and the valve is frequently activated in order to provide a haptic interface. So flow rate in a single on-off cycle is very difficult to precisely predict and the position estimation is thus difficult. To solve the problem, statistics method is applied in this paper.

This paper first provides a method to measure the pressure across the valve. Based on the pressure measurement method, this paper studies the possibility of precise speed control using the PWM method. Then, based on the results, explicit analysis is conducted. Finally, a control method is provided covering both speed control and position estimation using statistics method. With this control method, it is possible to combine the haptic control, speed control and position control together using only low-resolution pressure sensors.

2. STUDY ON PWM METHOD FOR SOLENOID VALVE – CYLINDER SYSTEM

2.1 Experimental System

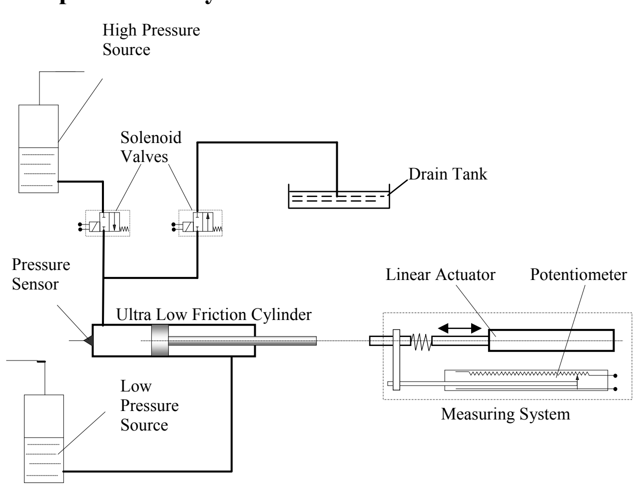

Figure 2-1 Experimental System Setup

The schematic diagram of the experimental system is given in Figure 2-1. An ultra-low friction cylinder represents an actuator/cell of the digital clay. Two solenoid on-off valves are used as the control valves, which have response times around 1.5ms. Two pressure sources, pressurized by regulated compressed air, are applied to drive the cylinder. Two low cost pressure sensors are used to measure the pressure difference across the inlet valve. Current research only deals with the inlet solenoid valve, so only the inlet valve is controlled using the PWM method.

A computer directly controls the whole system. A digital I/O card and a DAQ card provide the interfaces between the computer and the experimental system. To improve the performance, Real-time Linux is used as the operating system.

2.1.1 Measuring the Pressure across the Valve

One of the key parts of this research is the across valve pressure measurement method. Here, the across valve pressure means the pressure difference across the inlet valve.

A main drawback of solenoid valves is the big pressure surge caused by the sudden opening and closing, as shown in Figure 2-2. This big pressure surge can dramatically affect the pressure sensor when trying to detect the finger force acting on the cylinder rod tip. Low pass filtering successfully separates the pressure surges at the PWM frequency of 200 Hz from the finger force which is limited to 8 Hz or less.

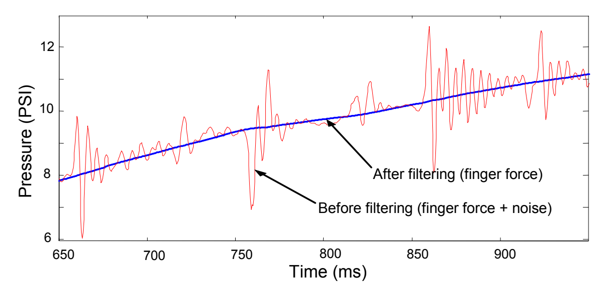

Figure 2-2 Efficacy of the Filter

Hence, all the research discussed in this paper is based on this filtered pressure feedback.

2.1.2 Measuring the Displacement of the Cylinder Rod

A measurement system is designed to measure the static displacement of the cylinder rod as shown in the lower right part of the figure 2-1. A linear actuator moves the measuring head left until it touches the cylinder rod. The spring between the measuring head and the linear actuator regulates the touching force. A potentiometer attached to the measuring head measures the displacement of the cylinder rod. There is no contact when the cylinder rod is moving. The measuring process only occurs after the cylinder rod stops.

2.2 Response to PWM Valve Actuation

The PWM base frequency is set to 200Hz, and 7 constant across-valve pressures were used as shown in figure 2-3. For each specified across valve pressure, 100 PWM duty cycles from 1% to 100% with an increment of 1% were applied on the inlet valve. After a certain PWM duty cycle is applied, the displacement of the cylinder rod is measured. The testing process is repeated several times for each specified across valve pressure ΔPv. The mean values are shown in Figure 2-3.

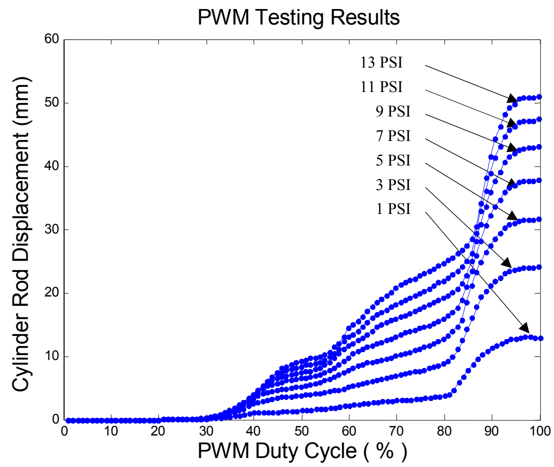

Figure 2-3 PWM Method Testing Result

The variance for 11 PSI is shown in figure 2-4 for illustration. Other results are quite similar to this.

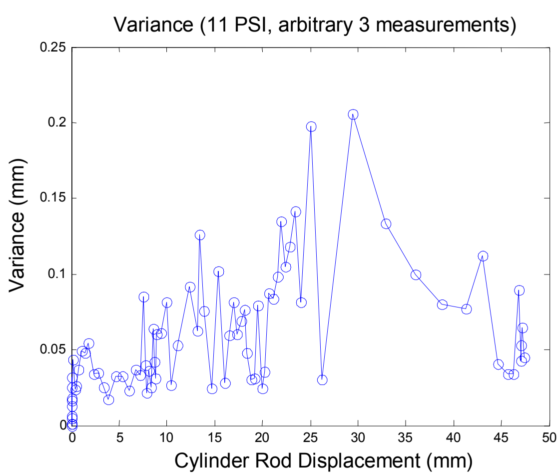

Figure 2-4 Variance for ΔPv =11 PSI

From figure 2-4, one can see that the testing noises are less than 0.05mm for small displacement (<5mm) and less than 2% for large displacement.

2.3 Trajectory of the Plunger of Solenoid Valve

Before advancing to the further experimental studies, theoretical analysis is conducted to gain more understanding of the test results above.

The valve used above has a structure shown in figure 2-5 (Only the NC port and the Common port are used). The free body diagram of the plunger is shown in figure 2-6.

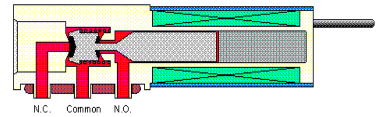

Figure 2-5 Structure of the Solenoid Valve

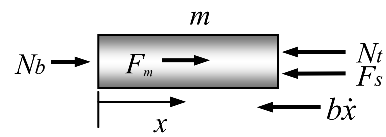

F_m	---	*Magnetic force*
F_s	---	*Spring return force*
N_t	---	*Resistant force when the plunger hits the right end*
N_b	---	*Resistant force when the plunger hits the left end*
b	---	*Damping ratio*

Figure 2-6. Free Body Diagram of the Plunger

From above free body diagram, the following equations are established:

$$F_m = F_s + N_t - N_b + m\ddot{x}(t) - b\dot{x};$$
$$F_s = F_0 + K_s x(t);$$
$$N_t = K_w < x - e >;$$
$$N_b = K_w < 0 - x >;$$

Where,

F_0	---	*Spring preload*
K_s	---	*Spring constant*
K_w	---	*Elastic module of the cousin*
N_b	---	*Plunger's stroke*
m	---	*Plunger's mass*

Note: <x - e> and <0 - x> are singular functions

The magnetic force F_m can be calculated using electrical magnetic theory as following:

$$F_m = \frac{B^2 S}{2\mu_0} = \frac{\mu_0 S N^2}{2(l+e)^2} * I^2$$

Where,

e	---	*Stroke of the plunger*
l	---	*Equivalent air gap*
N	---	*Rounds of the coil*
S	---	*Effect area of the magnetic effect on the plunger*
I	---	*Current of the coil*
μ_0	---	*Constant*
B	---	*Magnetic flux density*

The simulation result of the trajectory of plunger is plotted and shown in figure 2-7. (*By Matlab Simulink*)

Based on the simulation, following approximation is made to simplify further analysis: *Plunger moves at a constant speed when the coil is energized and de-energized.*

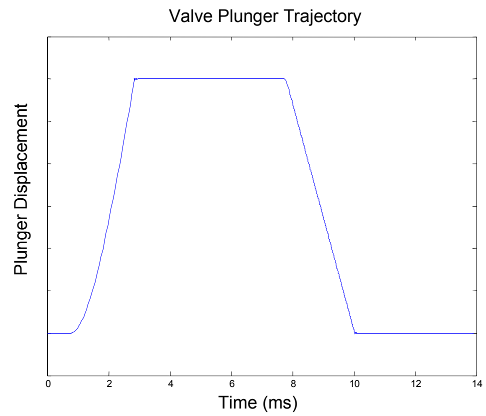

Figure 2-7 Simulated Valve Plunger Trajectory

2.4 Explicit Analytic Models for the Valve and Cylinder Motion

The whole working process of the plunger under the PWM driving method can be divided into four phases as shown in figure 2-8. The shape of the plunger trajectory will now be examined for each phase and an explicit analytical expression for flow and resulting piston motion will be derived. The method will be executed in detail for Phases I and II, and only the solution given for Phases III and IV. Note that in figure 2-8, there are two vertical axes. The one on the left is the measured cylinder rod displacement and the one on the right is the flow rate corresponding to the cylinder rod displacement (Cylinder rod moves at a constant speed).

Phase I:

When the valve is turned on, the plunger will not move immediately since it needs some time for the magnetic force to grow up and overcome the spring preload. So during phase I, the plunger does not move. That is why, when the PWM duty cycle is lower than 27%, the flow rate is zero as shown in figure 2-8. (When the PWM period is 5 milliseconds, 27% duty equal to an open time of 5*0.27 ≅ 1.4 milliseconds.)

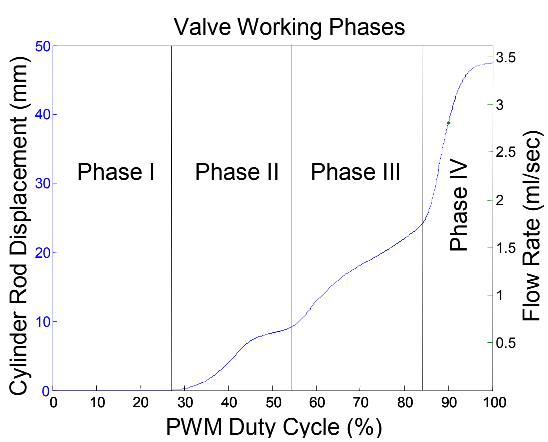

Figure 2-8 Solenoid Valve Working Phases Using PWM Method

Phase II:

After the magnetic force is bigger than the spring preload, the plunger starts to move and the valve begins to open. During this phase, the plunger does not reach the fully open position. Thus when the coil is de-energized, the plunger moves back immediately until fully closed. So during phase II, the valve is partially opened and fully closed. The plunger's trajectory under this phase is simulated and shown in figure 2-9a.

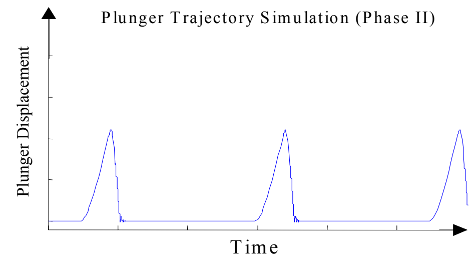

Figure 2-9a Plunger Trajectory Simulation under Phase II

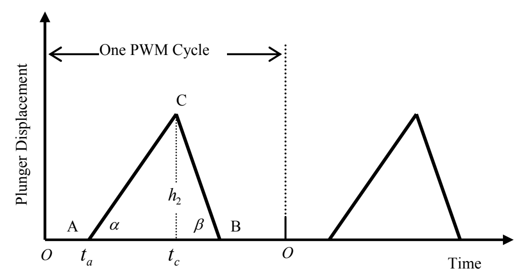

Figure 2-9b Approximated Plunger Trajectory

According to the fluid mechanics approximations commonly used for flow through sharp orifice, the flow rate

$$q = C_d \cdot \sqrt{\Delta P} \cdot A_o$$

Where, A_o is the area of the valve's orifice.

Cylinder rod displacement

$$y = \int \frac{q}{A_c} \cdot dt$$

Where, A_c is the area of the cylinder piston.

So the vertical coordinate of a point on the displacement-duty curve in figure 2-8 can be calculated as:

$$y = K_1 \cdot \int \frac{q}{A_c} \cdot dt = K_1 \cdot \int \frac{C_d \cdot \sqrt{\Delta P} \cdot A_o}{A_c} \cdot dt$$

$$= K \cdot \int x \cdot dt$$

Where :

$$K = \frac{C_d \cdot \sqrt{\Delta P} \cdot K_2 \cdot K_1}{A_c}$$

x	---	*Plunger displacement*
K_1	---	*Number of the PWM cycles in 1 second*
K_2	---	*Constant equals to* A_o / x
C_d	---	*Discharge coefficient*

For a given point on the displacement-duty curve, K_1, K_2 and C_d are constants, so K is constant.

$\int x \cdot dt$ is the area enclosed by the plunger trajectory and the horizontal axis (time axis) as shown in figure 2-9b. So, the vertical coordinate of a point on the displacement-duty curve during phase II can be calculated as below:

$$\begin{aligned}
y &= K \cdot S_{II} = K \cdot Area \quad of \quad \Delta ABC \\
&= K \cdot \frac{1}{2} \cdot h_2 \cdot \overline{AB} \\
&= K \cdot \frac{1}{2} \cdot (t_c - t_a) \cdot \tan\alpha \cdot [(t_c - t_a) + \frac{(t_c - t_a)\cdot \tan\alpha}{\tan\beta}] \\
&= K \cdot \frac{1}{2} \cdot (t_c - t_a)^2 \cdot \tan\alpha \cdot [1 + \frac{\tan\alpha}{\tan\beta}] \\
&= C_{II} \cdot (t_c - t_a)^2
\end{aligned}$$

$$where: \quad C_{II} = K \cdot \frac{1}{2} \cdot \tan\alpha \cdot [1 + \frac{\tan\alpha}{\tan\beta}]$$

Where,

0	---	*Time that the valve is energized, and also is the beginning of a PWM cycle*
t_a	---	*Time that the plunger begins to move*
t_c	---	*Time that the valve is de-energized*
α, β	---	*Angles as shown in figure 2-9b*

In following analysis, above notation always holds.

Phase III:

When the open time is long enough, the plunger will reach the right end (figure 2-5). After the plunger hits the right end, the magnetic energy starts to store in the coil. So when the coil is de-energized, the plunger will not move back until the energy stored in the coil is dissipated to certain amount. Thus there is a delay before the plunger starts to move back (CD in figure 2-10b). In phase III, the plunger is fully opened and fully closed.

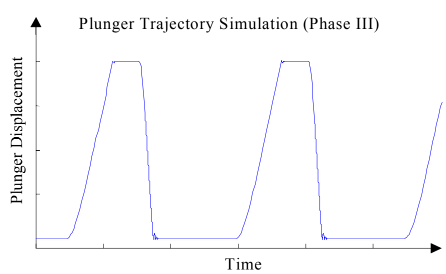

Figure 2-10a Plunger Trajectory Simulation under Phase III

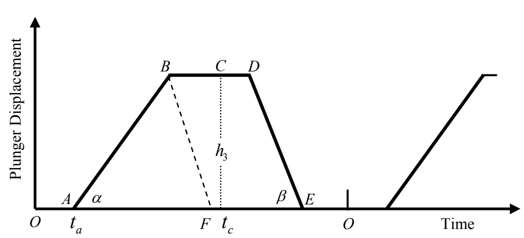

Figure 2-10b Approximated Plunger Trajectory

The vertical coordinate of a point on the displacement-duty curve during phase III can be calculated as (figure 2-10b):

$$\begin{aligned}
y &= K \cdot S_{III} = K \cdot (S_{\Delta ABF} + S_{BDEF}) \\
&= K \cdot (\frac{1}{2} \cdot h_3 \cdot \overline{AF} + h_3 \cdot \overline{BD}) \\
&= C_{II} + K \cdot h_3 \cdot [(t_c - t_b) + f(t_c - t_b)]
\end{aligned}$$

$$where: \quad C_{II} = K \cdot \frac{1}{2} \cdot h_3 \cdot \overline{AF}$$

Here $f(t_c\text{-}t_b)$ is a function describing the closing time delay due to the coil magnetic energy storage. So when t_c is bigger than a certain value, due to the saturation,

$$f(t_c - t_b) = C_m = \text{Constant.}$$

Thus,
$$y' = C_{II}' + K \cdot h_3 \cdot (t_c - t_b)$$
$$where \quad C_{II}' = C_{II} + K \cdot h_3 \cdot C_m$$

This can be seen in the figure 2-8. At the end of phase III, the slope of the curve is approximately constant.

Phase IV

During phase IV, as the PWM duty cycle increases, the plunger is pulled to open again by the magnetic force before it reaches the close position. So in phase IV, the valve is fully opened and partially closed.

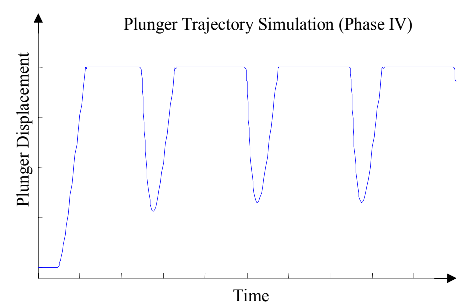

Figure 2-11a Plunger Trajectory Simulation under Phase IV

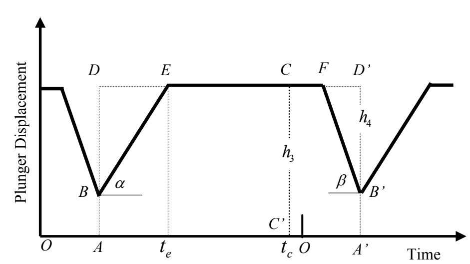

Figure 2-11b. Approximated Plunger Trajectory

The vertical value of the point on the curve in phase IV can be calculated as following:

$$
\begin{aligned}
y &= K \cdot S_{IV} = K \cdot (S_{ADD'A'} - S_{\Delta BDE} - S_{\Delta FD'B'}) \\
&= K \cdot (h_3 \cdot \overline{AA'} - \frac{1}{2} \cdot h_4 \cdot \overline{DE} - \frac{1}{2} \cdot h_4 \cdot \overline{FD'}) \\
&= C_{III} - C_{IV} \cdot (p - t_c - c_m)^2 \\
& where: \\
& C_{III} = K \cdot h_3 \cdot p \\
& C_{IV} = K \cdot \frac{1}{2} \cdot \tan^2 \beta (\frac{1}{\tan\alpha} + \frac{1}{\tan\beta})
\end{aligned}
$$

2.5 Data Process and Result

Above analysis provides an approximate calculation and explanation of the valve working behaviors under PWM. The actual curve is affected by a lot of factors. For example, the actual plunger-moving trajectory is not a straight line as approximated above, etc. Above analysis is only used as a guideline when processing the data, such as applying the curve fitting to get rid of the noise and uncertain measurement errors. By applying curve fitting based on previous analytical plunger working models, a chart of the flow rate under different across valve pressures is constructed and shown in figure 2-12.

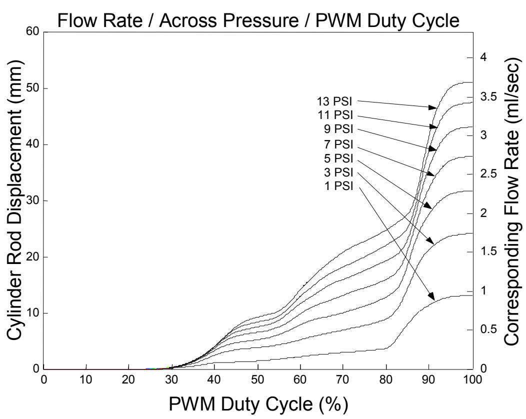

Figure 2-12 Curve Fit Using Model Result

3. SPEED AND POSITION CONTROL USING PWM

3.1 Reverse Process

Due to the complexity of the valve behaviors under PWM control, the lookup table method is adopted to realize the control. The lookup table is built as follows:

1. Construct a table consisting of duty-flow relations/curves corresponding to different across-valve pressure as shown in figure 2-12
2. Divide each curve by the square root of its corresponding across pressure (figure 3-1)
3. Reverse above duty-flow table to form a flow-duty table (figure 3-2)

The lookup table is used as follows:

1. Measure the current across valve pressure ΔP .
2. Calculate the duty-flow curve corresponding to ΔP using linear interpolation.
3. Multiply the interpolated desired duty-flow curve by $\sqrt{\Delta P}$.
4. Use the curve calculated in step 3 to find the PWM duty cycle according to the required flow rate or speed.

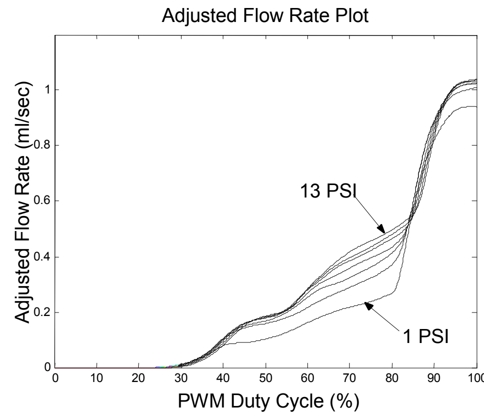

Figure 3-1 Adjusted Flow Rate (divided by $\sqrt{\Delta P}$)

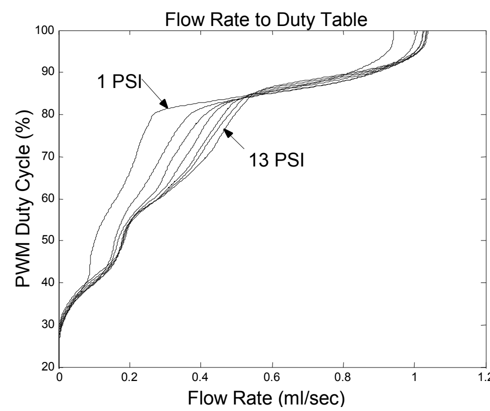

Figure 3-2 Table of Flow Rate to Duty

3.2 Control system structure & testing system

The general control structure of the speed and position control using PWM is shown in figure 3-3.

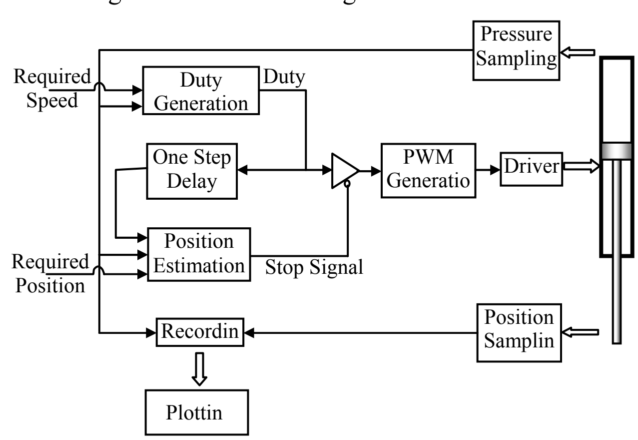

Figure 3-3 Structure of Speed and Position Control Using PWM

A testing system is set up as shown in figure 3-4 to test the proposed control method.

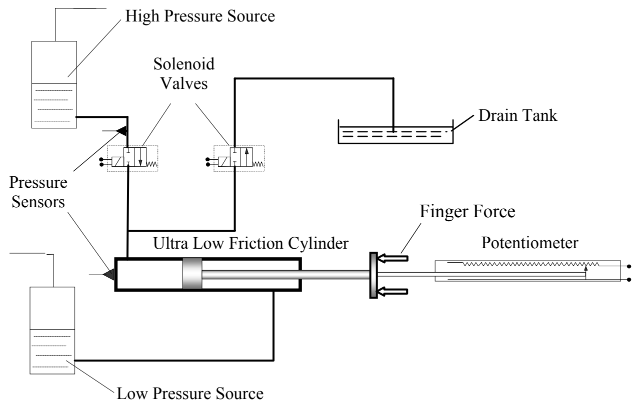

Figure 3-4 Testing System for Control Using PWM

3.3 Results

The testing is performed using the following devices and parameters: (table 3-1)

Pressure Sensor	Honeywell, 40PC015G2A, 0-15 PSI
Valve	The Lee, LHDA1223111H solenoid, 1.5 ms response time
Cylinder	Airpot, E9D5.0S, Ultra-low friction

Parameter	Value	Unit
Required Displacement	62.31	mm
Required Speed	12.46	mm/sec
PWM Base Frequency	200	Hz
PWM Duty Cycle Refresh Rate	40	Hz
Sampling Rate	20	kHz
Data Recording Rate	40	Hz
High-pressure Source	13.5	PSI
Low-pressure Source	2.5	PSI

Table 3-1 Parameters Used in Testing

3.4.1 Result for Zero Finger Force

The response of the testing system under zero finger force is shown in figure 3-5a. An ideal displacement is provided for reference (the dashed line drawn with slope equals to the required speed and ends at the required displacement). The across valve pressure is sampled by two pressure sensors (figure 3-4).

From figure 3-5a, one can see that the measured displacement overlaps the ideal displacement. Further more, the absolute error is plotted vs. ideal cylinder rod displacement (figure 3-5b). The absolute displacement error equals to (Measured Data – Ideal Data).

The result shows that the absolute displacement error is less than ±0.2 mm (or ±0.5% at the required displacement 62.31mm).

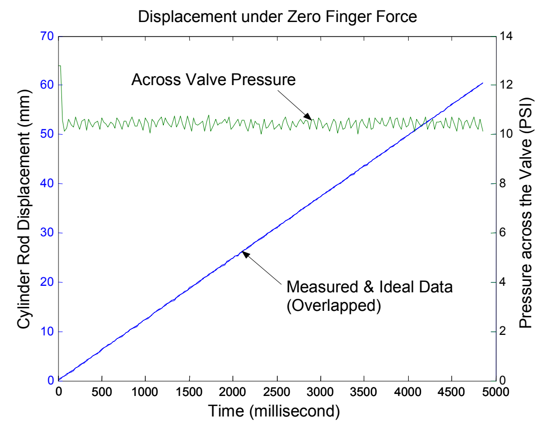

Figure 3-5a Cylinder Rod Displacement and Corresponding Across Valve Pressure when Finger Force is Zero

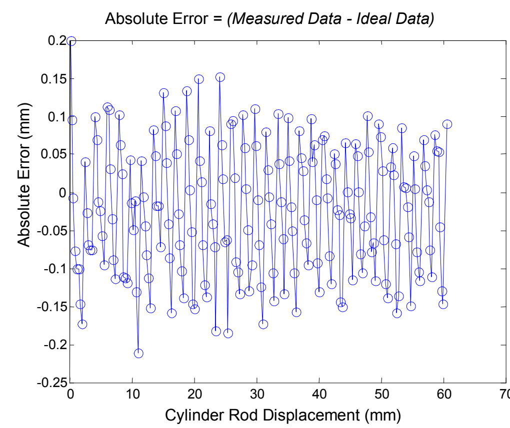

Figure 3-5b Absolute Displacement Error vs. Cylinder Rod Displacement when Finger Force is Zero

3.4.2 Result for varying finger force

Three independent tests are conducted with different types of varying finger force acting on the cylinder rod tip.

Result of the test with small amplitude (5 ~ 10.5 PSI) but high frequency finger force acting on the tip is shown in figure 3-6a. The corresponding absolute displacement error is shown in figure 3-6b. Result of the test with a comparatively bigger amplitude (3~10.5 PSI) but low frequency finger force is not shown due to the limitation of space. Comparing these two results, one can find that:

1. Varying finger force acting on the cylinder rod tip lowers speed and increases error.
2. The error increases when the finger force's amplitude increases.

Actually, so long as the finger force's frequency is lower than the refresh rate of the PWM duty (here is 40Hz), the finger force's frequency will not affect the error much.

Experiment also shows that even the cylinder rod is stopped by a large finger force for a while the relative displacement error is still less than 2 % after the cylinder rod is released.

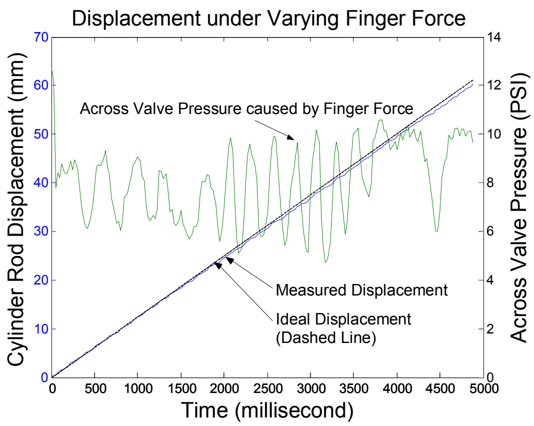

Figure 3-6a Cylinder Rod Displacement and Corresponding Across Valve Pressure (Caused by Finger Force)

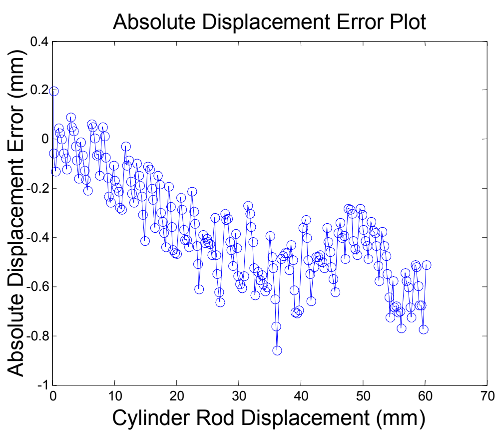

Figure 3-6b Absolute Displacement Error vs. Cylinder Rod Displacement (under Varying Finger Force)

4. FUTURE WORK

The control method proposed in this paper still has some small displacement and speed errors. In order to get rid of the building up of the errors, future work for the speed and position control will be (1) home position sensing, so every time the cylinder rod passes the home position, the displacement is calibrated and (2) External measurements for calibration and verification of shape.

5. CONCLUTION

Speed control and position estimation / control for discrete cells are critical for Digital Clay to provide dynamic shapes as well as a haptic interface. The proposed PWM control method is capable to control the on/off valve to achieve full range flow rate control as well as to precisely and robustly estimate and control displacement without any continuous position-sensing device.

ACKNOWLEDGMENTS

This work is supported by the U.S. National Science Foundation ITR grant IIS-0121663. The assistance of the co-investigators (Mark Allen, Ari Glezer, John Goldthwaite, David Rosen, Jarek Rossignac, Imme Ebert-Uphoff) and their colleagues and graduate students in the Schools of Mechanical Engineering and Electrical and Computer Engineering, and the College of Computing is gratefully acknowledged.

REFERENCES

[1]Linjama, M., Tammisto, J., Koskinen, K.T. & Vilenius, M. 2000. On/off position control of low-pressure water hydraulic cylinder using low-cost valves. In: Laneville, A. (ed.). Proceedings. Sixth Triennal International Symposium on Fluid Control, Measurement and Visualization, FLUCOME 2000, August 13-17, 2000, Sherbrooke, Canada. 6 p. (CD-ROM).

[2]IMAIZUMI, Tatsuhiko; OYAMA, Osamu; YOSHIMITSU, Toshihiro (2000) Study of Pneumatic Servo System Employing Solenoid Valve Instead of Proportional Valve by Keeping the Solenoid Valve Plunger to be Floating. In: FULCOME 2000 Conferenc, Sherbrooke, Canada .

[3]Q.Yang, Y.Kawakami, S.Kawai, PWM Position Control of a Pneumatic Cylinder, Journal of the Japan Hydraulics & Pneumatics Society, 27-6, 1995, 803/809.

[4]Linjama, M., Tammisto, J., Koskinen, K.T. & Vilenius, M. 2000. On/off position control of low-pressure water hydraulic cylinder using low-cost valves. In: Laneville, A. (ed.). Proceedings. Sixth Triennal International Symposium on Fluid Control, Measurement and Visualization, FLUCOME 2000, August 13-17, 2000, Sherbrooke, Canada. 6 p. (CD-ROM).

[5] O.Oyama, M.Harada, Pressure Servo System Using High Response Solenoid Valve: Journal of the Japan Hydraulics & Pneumatics Society, 20-4, 1989, 344/349.